Proceedings of the International Conference on Oxide Materials for Electronic Engineering (OMEE 2021)

Effect of Mechanochemical and Microwave Modification of SnO_2 Nanomaterials on Properties of Hydrogen Sensors

I. Matushko[a], S. Khalameida[b,*], M. Samsonenko[b], V. Sydorchuk[b], L. Oleksenko[a,c], N. Maksymovych[a], O. Khyzhun[d] and I. Kuraeva[c]

[a] *Taras Shevchenko National University of Kyiv, Department of Chemistry, Volodymyrska str., 64/1, 01033 Kyiv, Ukraine*
[b] *Institute for Sorption and Problems of Endoecology, NAS of Ukraine, Gen. Naumov str., 13, 03164 Kyiv, Ukraine*
[c] *The M.P. Semenenko Institute of Geochemistry, Mineralogy and Ore Formation, NAS of Ukraine, Krzhizhanovsky str., 3, 03142 Kyiv, Ukraine*
[d] *The I.M. Frantsevich Institute for Problems of Materials Science, NAS of Ukraine, Palladina ave., 34, 03142 Kyiv, Ukraine*

Doi: 10.12693/APhysPolA.141.247 *e-mail: svkhal@ukr.net

Tin dioxide was modified via mechanochemical and microwave treatments in order to obtain a mesoporous structure. Samples treated in water possess a thermostable crystal and porous structure. As a result, the samples modified in this way retain a large specific surface area after the manufacture of the sensor. Microwave treatment of SnO_2 gel at 270°C is more promising for the creation of sensitive semiconductor sensors.

topics: tin dioxide, mechanochemical and microwave treatments, porous structure, hydrogen sensors.

1. Introduction

Nowadays, the synthesis and study of the unique functional properties of nanomaterials are one of the promising areas of research due to their characteristics and wide possibilities of applications. In particular, it is possible to create new, highly sensitive gas sensors based on semiconductor oxides that are capable to detect toxic and explosive gases of various nature at relatively low operating temperatures [1–3].

Tin dioxide is an n-type semiconductor ($E = 3.6$–4.0 eV [2]) that is widely used to create adsorption semiconductor gas sensors purposed to control ambient air [4]. Its morphology and structure-adsorption properties largely depend on the gas-sensitive properties of the sensors. High-temperature calcination is a necessary stage in the fabrication of the gas-sensitive sensor layers based on nanosized SnO_2. The latter can cause the enlargement of particles of the sensor material, decrease in its specific surface, change the porous structure and, consequently, lead to a change in the parameters of the sensors built on their base [4]. These indicated physicochemical characteristics can be changed by various methods of preparing nanomaterials. It is known that the modification of oxides under hydrothermal conditions, including via mechanochemical and microwave treatments, allows to create a larger porous and more uniform structure, which does not sinter at high temperatures while maintaining sufficiently high specific surface area and lesser crystallite sizes of nanomaterials [5].

The aim of this work is to study the effect of mechanochemical and microwave modification on the specific surface area, porous structure of tin dioxide and the functional characteristics of the corresponding sensors with gas-sensitive layers based on modified SnO_2.

2. Experimental

2.1. Synthesis and modification

Tin dioxide was prepared and modified as described in [6]. Thus, the initial sample (SnO_2-Init) was obtained by heterogeneous precipitation at pH 4 from the $SnCl_4 \cdot 5H_2O$ solution. Mechanochemical treatment (MChT) of dried xerogel was carried out using a planetary ball mill "Pulverisette-7" ("Fritsch", Germany) in air and water for 0.5 h at 600 rpm (samples MChT-air and MChT-H_2O, respectively). A wet gel of SnO_2 was subjected

TABLE I

Parameters of porous structure and particle size for modified samples.

Samples	S [m^2/g]	V_Σ [cm^3/g]	V_{me} [cm^3/g]	V_{mi} [cm^3/g]	d_{me} [nm]	D_{TEM} [nm]	D_{110} [nm]
Init	178	0.05	0.02	0.03	2.3	11	2.1
Init-550	26	0.11	0.11	–	5.6	31	11.7
MChT-air	136	0.07	0.03	0.04	2.4	8	2.3
MChT-air-550	29	0.09	0.09	–	6.5	29	9.8
MChT-H_2O	158	0.27	0.04	0.03	3.8	7	2.1
MChT-H_2O-550	38	0.23	0.11	–	6.6	25	10.1
MChT-H_2O-450	60	0.26	0.16	–	3.8	9	6.2
MChT-H_2O-450-620	52	0.24	0.12	–	5.6	11	9.0
MChT-H_2O-450-Co-620	37	0.23	0.13	–	6.6	17	9.4
MWT	165	0.23	0.23	–	6.5	14	4.2
MWT-450	84	0.23	0.23	–	6.7	18	5.4
MWT-450-620	63	0.14	0.14	–	6.5	11	6.1
MWT-450-Co-620	61	0.15	0.15	–	6.5	13	8.6

to microwave treatment (MWT) at 270°C using a high-pressure reactor "NANO 2000" ("Plazmotronika", Poland). MWT compares favourably with conventional HTT since it takes much less time to achieve the same result [7]. All samples were calcined in air at 450 and 550°C for 3 h — the temperature is indicated in the designation of the corresponding samples in Table I.

2.2. Physical–chemical characterization

Phase composition of the initial and doped samples was analyzed on a Philips PW1830 diffractometer with Cu K_α radiation. Adsorption–desorption isotherms of nitrogen were recorded using an ASAP 2405N analyzer ("Micromeritics Instrument Corp"). On their basis, the specific surface areas S, the micropores volume V_{mi}, the mesopores volume V_{me} and the mesopores diameter d_{me} were calculated. The total pore volume V_Σ was determined by ethanol impregnation of the granules of the materials that were dried at 150°C.

Morphology for the obtained samples was investigated using a JEM 1230 transmission electron microscope (JEOL). Histograms of the particle size distribution were plotted using an "ImageJ" software.

Determination of cobalt content in samples was performed using a commercial XRF spectrometer (Elvax Plus) with Rh-anode, 800 μN Al filter, resolution of 0.14 keV (FWHM), and a 7.4 mm collimator. The source operated at the voltage of 35 kV. The real analysis time for each spectrum was 100 s.

X-ray photoelectron spectroscopy (XPS) was used to test samples containing cobalt. The XPS spectra were measured with a UHV-Analysis-System (SPECS, Germany). Interpretation of obtained results was carried out using the works [8, 9].

2.3. Sensor preparation and measurements of its properties

The sensor of size $2 \times 2 \times 0.3$ mm^3 consisted of a ceramic plate with a heater on one side of the plate and measuring contacts on the opposite side of the plate. The semiconductor sensors were made using thick-film technology. For this purpose, a paste using a modified SnO_2 and 3% aqueous solution of carboxymethylcellulose was deposited on the ceramic plate between the measuring contacts. The sensor plates were dried for 1 h in air at room temperature for 1 h at 90°C. Introduction of cobalt additives was carried out by impregnating it with a hydrochloric acid solution (0.02 N) and $CoCl_2$ solution (6×10^{-2} M). The sensors were then sintered in a high-temperature oven up to 620 °C [10]. The cobalt content in the gas sensitive nanosized Co–SnO_2 material after the MChT modification was 0.32 wt% and in the Co–SnO_2 nanomaterial after MWT modification — 0.40 wt%.

The measure of sensitivity (Y) was the ratio of the value of the electrical resistance of the sensor in the air (R_0) to the resistance in the presence of 40 ppm of hydrogen in the air (R_{H_2}), namely $Y = R_0/R_{H_2}$. The stability of the sensors was investigated by measuring the sensor signal at hydrogen-air mixture (40 ppm H_2) every hour during a day. The temperature of the sensors was determined by an optical pyrometer.

3. Results and discussion

The initial sample of SnO_2 has a micro–mesoporous structure with a predominance of micropores and with the size of the mesopores at the border with microporosity. The initial sample was subjected to milling by MChT in air and water, and microwave treatment (MWT) as

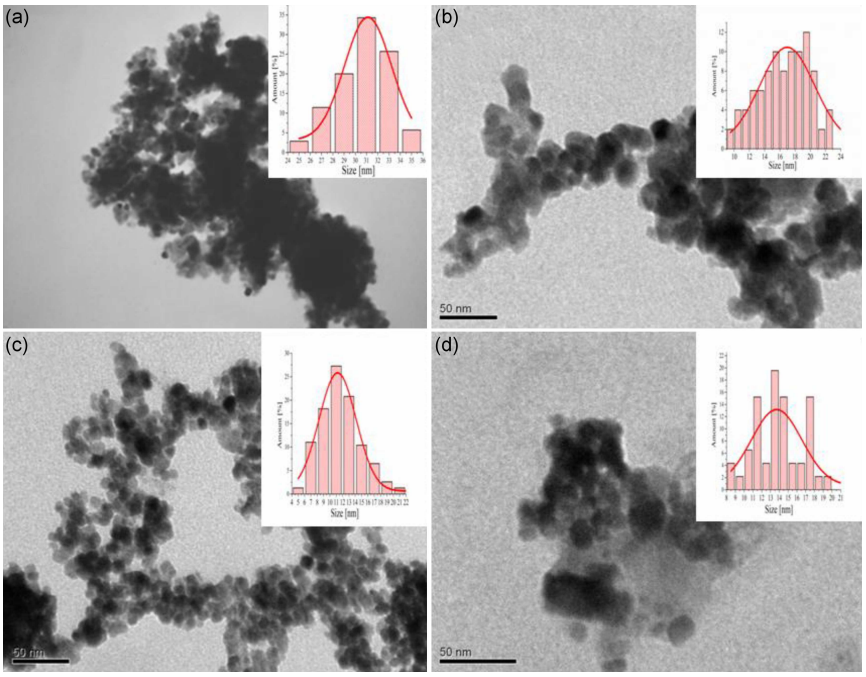

Fig. 1. TEM images and histograms of the particle size distribution for the samples (a) Init-450, (b) MWT-450, (c) MWT-450-620, (d) MWT-450-Co-620.

a wet gel under hydrothermal conditions. As shown earlier [5, 7], MChT in water and MWT cause a reduction in specific surface area and a sharp increase of the total pore volume and mesopore size (Table I). It is important that the contribution of the different types of pores in the total pore volume varies significantly. Consequently, the sample becomes uniformly mesoporous after MWT, while a bi-porous, namely meso–macroporous structure is formed for the MChT-H_2O sample. The presence of macropores with a volume of 0.1–0.2 cm^3/g is confirmed by the excess of the total pore volume V_Σ over the sum of the volumes of micro- and mesopores.

As a result, the preliminary MWT and MChT in water promote a noticeable increase in the specific surface area of the annealed samples compared with that for the same initial sample. Their values are 44 m^2/g for the initial sample (without any pretreatment) and 60 and 84 m^2/g for MChT-H_2O-450 and MWT-450 samples, respectively. Therefore, the highest thermostability of the specific surface area has the sample after MWT, which maintains a high surface value after preparation of sensor at 620°C with and without cobalt (61 and 63 m^2/g, respectively). It is noteworthy that the size of the mesopores does not change for this sample even after calcination at 620°C, although the volume of mesopores decreases significantly under these conditions. The obtained gain of the specific surface area in comparison with the initial sample is due to the fact that the samples modified in water have a larger mesopore size and contain macropores, and therefore sinter to lesser extent during annealing [11, 12]. At the same time, the MChT-air sample, which contains more micropores and fewer mesopores, is sintered more strongly. As a result, its specific surface area decreases almost as well as in the calcined initial sample. The latter is obviously due to the introduction of defects in the SnO_2 structure during dry milling. It is well known that solids with defects are easily sintered [12].

An important characteristic of oxide materials for gas sensors is also their stability toward crystallites and particle growth during annealing [8, 13]. It is believed that tin dioxide with a crystallite size below 10 nm shows higher sensitivity [13, 14]. The initial SnO_2 sample is low-crystalline cassiterite (ICSD No. 84576) [5, 7]. It has a crystallite size of about 2 nm according to calculation using the Sherrer formula (Table I). Its preliminary modification with MChT does not change the degree of SnO_2 crystallinity, while MWT improves it (Fig. 1). This is expressed in particular in an increase of the crystallite size up to 4 nm. The latter is due to Ostwald ripening processes taking place under hydrothermal conditions [6, 15]. Next calcination promotes crystallite growth, which is less for pre-modified samples, especially after MWT.

The examples of transmission electron microscope (TEM) images are presented in Fig. 1. One can see that the samples consist of consolidated spherical particles 5–30 nm in size. Noteworthy is the excess of particle size obtained from the TEM data (D_{TEM}) over the crystallite size calculated from the XRD results (D_{110}). This indicates aggregation of primary crystallites which is characteristic for porous solids. As a result, the average

TABLE II

The values of the electrical resistance in air at different temperatures for the sensors based on various sensitive materials.

Sensor temperature [°C]	R_0 [kΩ]			
	Materials for the gas sensitive layers of the sensors			
	MChT-H_2O-450-620	MWT-450-620	MChT-H_2O-450-Co-620	MWT-450-Co-620
185	9570	8310	4600	3700
223	5993	6015	2220	1569
259	7860	9668	1110	1207
293	10110	12298	1000	1170
323	6960	9133	960	1023
350	5555	6790	835	1100
380	4990	5398	811	1096
405	2415	2350	760	765

TABLE III

Sensitivity to H_2 (40 ppm) at different temperatures for the sensors obtained from different materials.

Sensor temperature [°C]	R_0/R_{H_2}			
	Materials for the gas sensitive layers of the sensors			
	MChT-H_2O-450-620	MWT-450-620	MChT-H_2O-450-Co-620	MWT-450-Co-620
185	1.04	1.02	1.01	1.02
223	1.29	1.33	1.05	1.39
259	2.59	2.94	2.12	3.02
293	3.60	4.00	4.30	7.23
323	3.20	3.60	4.82	5.70
350	2.27	3.30	4.10	4.65
380	1.81	3.00	3.29	3.89
405	1.36	2.53	2.60	2.75

particle size is 9 nm for the MChT-H_2O-450 sample and 18 nm for the MWT-450 sample. The particle size increases for "mechanochemical" sample but decreases for "microwave" sample after sensor fabrication that includes annealing at 620°C.

Figure 2 presents the survey XPS spectra of the Co-containing samples under study. The main contributors to the spectra are oxygen and tin with smaller additions of adsorbed carbon. Despite the small content (0.3–0.4 wt%), traces of cobalt are detected but the most informative Co $2p_{3/2}$ spectrum superimposes the oxygen Auger KL_1L_1 line. Furthermore, rather intensive XPS Sn $3p_{1/2}$ core-level line is positioned very close to the Co $2p_{3/2}$ line. Therefore, it is not possible to determine its content in the surface layer. The values of binding energy (BE) for Co $2p_{3/2}$ are 780.6 and 780.0 eV for samples MWT-450-Co-620 and MChT-H_2O-Co-620, respectively. This corresponds to the Co^{2+} state of cobalt [9, 16]. The BEs for O 1*s* electrons (530–531 eV) and Sn $3d_{5/2}$ core-level electrons (486–487 eV) are attributed to O^{2-} and Sn^{4+}, respectively.

Tables II and III present results of the study of the semiconductor sensors S-MChT-H_2O, S-MWT, S-MChT-H_2O-Co and S-MWT-Co. Gas sensitive layers of the sensors were made on the basis of the synthesized materials MChT-H_2O-450, MWT-450, MChT-H_2O-450-Co and MWT-450-Co, respectively. To understand the results of the studied semiconductor sensors, we consider the sensitive layers as heterogeneous catalysts and the reaction between the adsorbed oxygen from the air and the analyzed gas running on the surface of these catalysts [17, 18].

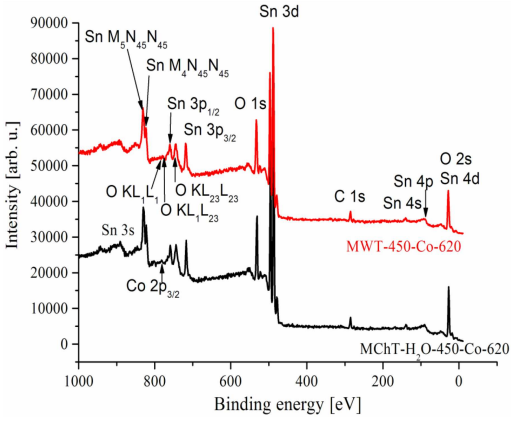

Fig. 2. Survey XPS spectra for Co-containing samples.

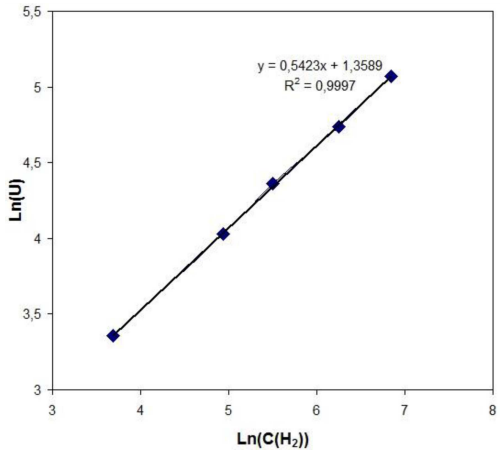

Fig. 3. Dependence of the signal of the optimal sensor based on MWT-450-Co nanomaterial on the hydrogen concentration in the logarithmic scale. The temperature of the sensor is 293°C.

It was found for the cobalt-free sensors (Table II) that rise in their temperature probably leads to an increase in the amount of the chemisorbed oxygen. As a result, an increase in their resistances is observed, which reaches a maximum at temperature of 293°C. A further increase in the sensor temperature probably leads to the desorption of oxygen from the surface and a decrease of sensors electrical resistances (Table II).

The obtained experimental data (Table II) shows that the character of the change in the values of electrical resistance of the sensor corresponds to the character of changes in their sensitivity (Table III). The maximum sensitivity for these sensors is also achieved at 293°C. Under these temperature conditions, the sensitivity values for sensors with a gas-sensitive layers based on MWT-450 material are slightly higher than for sensors with a gas-sensitive layer material based on MChT-H_2O-450 (Table III). This is due to larger active surface of the first material (Table I).

As can be seen from the data presented in Table III, the values of the sensitivity of sensors with cobalt as well as for sensors without cobalt, exhibit a maximum as a function of temperature. The values of the sensitivity are much higher for sensors with Co than for sensors without Co additive. This confirms the role of cobalt as a known active component of the catalyst for the catalytic oxidation reactions [19], in particular for the oxidation of hydrogen [8]. Cobalt increases the rate of H_2 oxidation and in this way increases the sensitivity of both sensors. This was also observed for cobalt-containing sensors based on tin dioxide obtained by other methods [8, 20]. It should be noted that for cobalt-containing sensors from MChT-H_2O-450-Co, the values of their sensitivity are smaller than for sensors obtained with MWT-450-Co material. This is consistent with a larger value of the active surface of the sensitive layer material of the last sensors (Table I). The addition of cobalt to gas-sensitive materials obtained by both studied methods significantly reduces the electrical resistances of the sensors (Table II). Such low resistance of sensors is able to mask the influences of processes occurring on the surface of the gas sensitive material (oxygen chemisorption). Therefore, for the Co-containing sensors there is no relationship between the experimentally established change in their electrical resistance and the sensitivities of the sensors.

TABLE IV

Stability of the sensor signal during a day operation for the sensor S-MWT-450-Co-620 at 293°C.

Time [h]	Sensor signal [mV]
1	138.3
2	142.73
3	141.77
4	144.85
5	138.88
6	143.50
7	142.15
8	138.69

It was found that the Co-containing sensor S-MWT-450-Co-620 is stable. The values of the sensor signals working at 360°C in the presence of 40 ppm H_2 practically did not change during one day of continuous sensor operation (Table IV).

It was found that the sensor obtained using the MWT-450-Co nanomaterial is optimal. It is capable to measure hydrogen in a wide range of its concentrations (40–1000 ppm). The dependence of the sensor signal on the concentration of hydrogen in the logarithmic scale is linear (Fig. 3), which allows to carry out the periodic calibration of the sensors at two concentrations of hydrogen.

4. Conclusions

It is found that microwave and mechanochemical treatments of the semiconductor materials based on SnO_2 in water affects the structural parameters. In particular, these kinds of modifications allow to form meso–macroporous structures that are stable at high temperature at which sensors are fabricated. Also, the particle size of modified SnO_2 materials is within the range of 11–17 nm, even after calcination at 620°C. These physicochemical characteristics of modified materials determine the improved gas-sensitive properties of the sensors created on their basis. Microwave treatment of SnO_2 in the form of a wet gel at temperature of 270°C is more promising for the fabrication of sensitive semiconductor sensors than mechanochemical sensors. In particular, sensors based on SnO_2 after microwave treatment are capable to measure hydrogen in the concentration range of 40–1000 ppm.

References

[1] A. Dey, *Mater. Sci. Eng. B* **229**, 206 (2018).

[2] G. Fedorenko, L. Oleksenko, N. Maksymovych, *Adv. Mat. Sci. Eng.* **2019**, 5190235 (2019).

[3] L.P. Oleksenko, N.P. Maksymovych, E.V. Sokovykh, I.P. Matushko, *Theor. Exp. Chem.* **50**, 115 (2014).

[4] G. Li, X.-H. Zhang, S. Kawi, *Sens. Actuators B* **60**, 64 (1999).

[5] S. Khalameida, M. Samsonenko, J. Skubiszewska-Zięba, O. Zakutevskyy, *Adsorp. Sci. Technol.* **35**, 853 (2017).

[6] G. Yang, S.-J. Park, *Materials* **12**, 1177 (2019).

[7] M. Samsonenko, O. Zakutevskyy, S. Khalameida, B. Charmas, J. Skubiszewska-Zięba, *Adsorption* **25**, 451 (2019).

[8] L.P. Oleksenko, N.P. Maksymovych, I.P. Matushko, A.I. Buvailo, N.M. Derkachenko, *Russ. J. Phys. Chem. A* **87**, 265 (2013).

[9] S.C. Petitto, E.M. Marsh, G.A. Carson, M.A. Langell, *J. Mol. Catal. A* **28**, 49 (2008).

[10] L.P. Oleksenko, G.V. Fedorenko, N.P. Maksymovych, I.P. Matushko, *Func. Mat.* **25**, 741 (2018).

[11] K. Lu, W. Li, B. Chen, *Eng.Mater.* **35**, 115 (2013).

[12] I. Prochazka, J. Cizek, O. Melikhova, W. Anwand, T.E. Konstantinova, I.A. Danilenko, *Diffusion Foundations* **1**, 155 (2014).

[13] A. Rothschild, Y. Komem, *J. Appl. Phys.* **95**, 6374 (2004).

[14] S. Seal, S. Shukla, *J. Miner. Met. Mater. Soc.* **54**, 35 (2002).

[15] G.J. Wilson, A.S. Matijasevich, D.R.G. Mitchell, J.C. Schulz, G.D. Will, *Langmuir* **22**, 2016 (2006).

[16] S. Malvankar, S. Doke, R. Gahlaut, E. Martinez-Teran, A.A. El-Gendy, U. Deshpande, S. Mahamuni, *J. Electron. Mater.* **49**, 1872 (2020).

[17] L.P. Oleksenko, G.V. Fedorenko, N.P. Maksymovych, *Theor. Exp. Chem.* **55**, 132 (2019).

[18] L. Oleksenko, G. Fedorenko, N. Maksymovych, *Res. Chem. Intermed.* **45**, 4101 (2019).

[19] L.P. Oleksenko, L.V. Lutsenko, *Russ. J. Phys. Chem. A* **87**, 180 (2013).

[20] L.P. Oleksenko, N.P. Maksimovich, L.V. Shuvar, I.P. Matushko, *Theor. Exp. Chem.* **49**, 310 (2013).